Mechanics & Industry **21**, 505 (2020)

https://doi.org/10.1051/meca/2020061

Mechanics & Industry

Available online at:
www.mechanics-industry.org

REGULAR ARTICLE

Comparative study of the effective parameters on residual stress relaxation in welded aluminum plates under cyclic loading

Yousef Ghaderi Dehkordi[1], Ali Pourkamali Anaraki[1,*], and Amir Reza Shahani[2]

[1] Department of Mechanical Engineering, Shahid Rajaee Teacher Training University, 16758-136 Tehran, Iran
[2] Faculty of Mechanical Engineering, K.N. Toosi University of Technology, 16765-3381 Tehran, Iran

Received: 27 March 2019 / Accepted: 23 June 2020

Abstract. The prediction of residual stress relaxation is essential to assess the safety of welded components. This paper aims to study the influence of various effective parameters on residual stress relaxation under cyclic loading. In this regard, a 3D finite element modeling is performed to determine the residual stress in welded aluminum plates. The accuracy of this analysis is verified through experiment. To study the plasticity effect on stress relaxation, two plasticity models are implemented: perfect plasticity and combined isotropic-kinematic hardening. Hence, cyclic plasticity characterization of the material is specified by low cycle fatigue tests. It is found that the perfect plasticity leads to greater stress relaxation. In order to propose an accurate model to compute the residual stress relaxation, the Taguchi L18 array with four 3-level factors and one 6-level is employed. Using statistical analysis, the order of factors based on their effect on stress relaxation is determined as mean stress, stress amplitude, initial residual stress, and number of cycles. In addition, the stress relaxation increases with an increase in mean stress and stress amplitude.

Keywords: Taguchi / stress relaxation / plasticity / cyclic load / aluminum

1 Introduction

Welding has been widely used in production and repair of components. Due to high-localized temperature during welding and subsequent rapid cooling, the tensile residual stress is developed in and near to the weld area, which can significantly reduces the life expectancy of structures [1–3]. To extend the service life of engineering structures, there are different methods to reduce the harmful tensile residual stress, such as the heat treatment [4,5], shot peening [6–8], and mechanical loading [9–23]. However, the welded structures tolerate the residual stress as well as the stress resulted by in-service mechanical loads. Therefore, to assess the safety of structures, it is necessary to take into account the residual stress redistribution. It is understood that when the total stress exceeds than the local yield stress of material, the residual stress relaxation occurs as a result of plastic deformation. To predict the plasticity, different constitutive models from simple elastic-perfectly plastic to more complicated rules have been developed. Some studies used the analytical method for modeling the residual stress relaxation [9–11]. Such methods typically make some simplifying assumptions and, as a result, were unable to accurately model the complexities involved with the 3D welding residual stress. Therefore, numerical method based on the finite element (FE) analysis has been developed. Yi and Lee [12] carried out the FE analysis to evaluate the residual stress relaxation in the steel welded plates under cyclic load. They considered the stress relaxation only on the axial direction. Moreover, they did not taken into account the material hardening. Barsoum [13], and Katsuyama and Onizawa [14] also studied the welding residual stress relaxation without cyclic plasticity modeling. They performed FE analysis based on the elastic-perfectly plastic behavior. Since these studies did not consider the cyclic plasticity hardening, the residual stress state was not accurately predicted. Katsuyama et al. [15] considered a bilinear stress–strain equation with linear kinematic hardening to study the welding residual stress relaxation under repeated loading. They observed that the higher loading caused the greater relaxation. Dattoma et al. [16] assumed the isotropic hardening behavior to predict the stress relaxation. They concluded that the stress relaxation occurs only in the first cycle. Their results revealed that the stress relaxation depends not only on the load amplitude but also on the load direction. Qian et al. [17] showed that the different types of steel exhibited very different residual stress relaxation behavior. Gannon et al. [18] used the constitutive model combined of perfectly

* e-mail: ali_pourkamali@srttu.edu

plastic behavior and the kinematic hardening model. They concluded that for shipbuilding steel, the kinematic hardening has a little influence on stress relaxation. They also showed that the residual stress reduction occurs entirely during the first cycle if the magnitude of the cyclic load is not subsequently exceeded. Cho and Lee [19] studied the interaction between the residual stress and cyclic loading in a welded steel pipe. They proposed a kinematic hardening model [20] to take into account the cyclic plastic strain. Their simulation indicated that the stress relaxation depends on the direction and magnitude of external load. Xie et al. [21] proposed a model to predict the residual stress relaxation in the welded plates based on the experimental and FE results. They used the combined isotropic and kinematic hardening in the constitutive model. Farajian et al. [22,23] measured the initial and relaxed residual stresses in the welded plates under cyclic load by means of X-ray method. They concluded that the stress relaxation occurs at the first loading cycle when the von Mises stress exceeds than the monotonic yield strength.

It is clear that the welding residual stress relaxation is a complex phenomenon, which depends upon a wide range of variables. Further, experimental design is a useful method to identify the effective parameters and their impacts on response variable. In this study, experimental design is done to study the characteristics of welding residual stress relaxation under cyclic load. First, a 3D FE model is developed to predict the initial residual stress. Moreover, to validate the model, the predicted residual stress was compared with the experimental result. Subsequently, the analysis is developed to apply the cyclic load, with various amplitudes and cycle numbers. The stress relaxation is highly dependent on the plasticity, particularly in metals that show strain hardening. To study the plasticity behavior on stress relaxation, two different models are used: (1) perfect plasticity, and (2) combined nonlinear isotropic-kinematic hardening. Hence, cyclic plasticity characterization of the material is specified by low cycle fatigue tests. In order to provide a simple analytical model for prediction the stress relaxation, the Taguchi L18 array with one 6-level factor and four 3-level factors is used. The specification of cyclic load and the initial welding residual stress were chosen as the design factors. Variance analysis is also performed to determine the impact and contribution of each factor on the residual stress relaxation.

2 Experimental procedure

The experimental procedure consists of two steps: material properties and specimen production, and residual stress measurement, as described below.

2.1 Material properties and specimen production

The experimental specimen was prepared through single-pass butt-welding of the 5000-series aluminum plates with length 350 mm, width 250 mm, and thickness 2 mm. The GTAW process was done with welding parameters given in Table 1. The thermal specifications [24] and the mechanical properties of the material versus to the temperature are plotted in Figure 1. Due to the high impact of yield strength on the welding residual stress, the mechanical properties were determined by high-temperature tensile test, based on the ASTM E 21 standard [25]. The specimen geometry, which was used in this test, is shown in Figure 2.

Table 1. Parameters of the welding process.

Current-AC (A)	Voltage (V)	Speed ($mm\,s^{-1}$)	Shielded gas
170	10	1.6	Argon

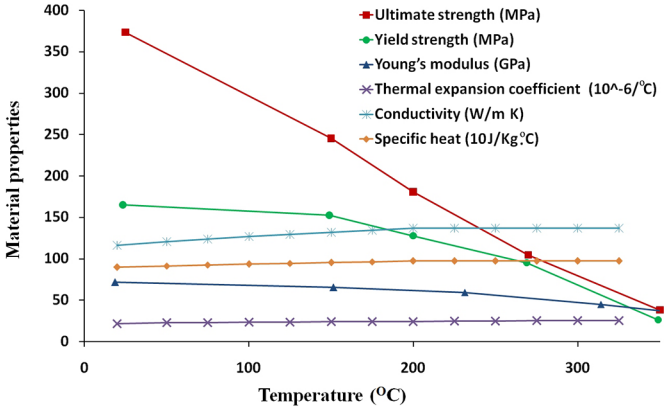

Fig. 1. Temperature-dependent properties of material.

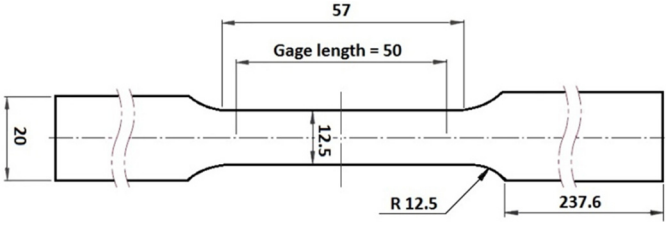

Fig. 2. Specimen geometry of high temperature tensile test [25].

2.2 Residual stress measurement

During the past years, various techniques have been developed to measure the residual stress in welded structures. Among these methods, the hole-drilling is a widely used technique. It offers advantages of good accuracy and reliability, standardized test procedure, and non-significant damage [26]. In this study, in order to verify the FE analysis, the welding residual stresses were measured through the incremental hole-drilling method. In this method, a small hole is drilled in an incremental number of steps and the corresponding strains are measured on the surface. The residual stresses are calculated with these measured strains. Hence, five strain gages of type rosette were bonded to the specimen surface as shown in Figure 3. The blind-holes with depth 1 mm were drilled precisely at the center of the rosette using

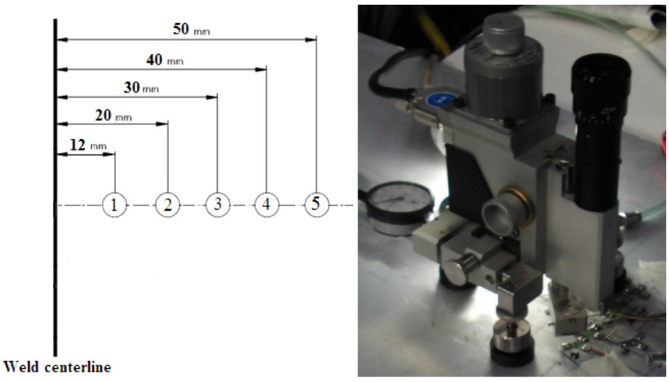

Fig. 3. Residual stress measurement (a) strain gauge position (b) drilling process.

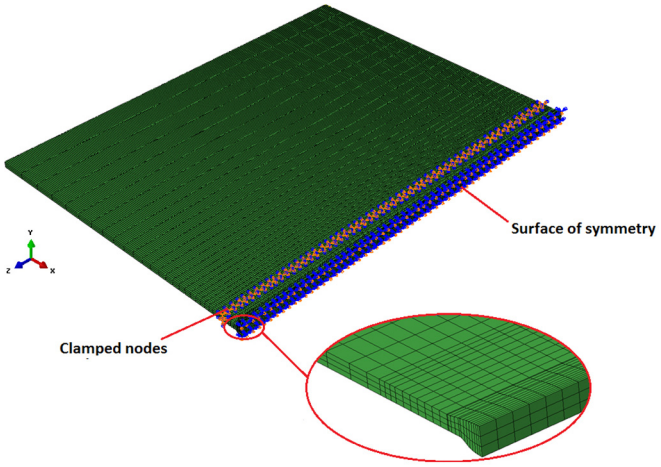

Fig. 4. FE model of the welding simulation.

Table 2. Stages of the welding simulation.

Stage number	Stage time (s)	Stage specification
Stage 1	219	Heating (welding time)
Stage 2	2500	Cooling
Stage 3	1	Releasing the clamps

an air-turbine at rotation speed 300,000 rpm, feed rate 0.2 mm/min, depth increment 0.05 mm, and delay time 5 seconds. The cutting tool was a tungsten carbide inverted cone end mill with 1.6 mm in diameter and six cutting edges.

The depth of each hole was 1 mm, being drilled in 20 steps 2.3 of 50 μm each.

3 Welding simulation of the butt-jointed plates

3.1 General consideration

The thermo-elasto-plastic analysis was performed based on the couple method between the thermal and mechanical solutions. The analysis was done in three stages as seen in Table 2. The 3D FE model was constructed and meshed using ABAQUS software, as shown in Figure 4. For the boundary condition, the nodes at distance 16 mm from the weld centerline were fixed due to the clamps of welding machine, and then released due to removing the clamps. The thermal gradient is highest at the welded zone, so the finer mesh size was used near the weld. The identical geometry and mesh configurations were utilized in the thermal and mechanical analyses. Whereas, the element types DC3D20 and C3D20R were used in the thermal and mechanical analyses, respectively.

3.2 Thermal analysis

For the heat source simulation, the most popular model, proposed by Goldak et al. [27] was used. In this model,

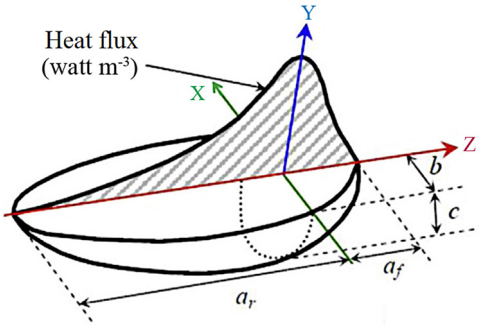

Fig. 5. Double-ellipsoidal heat source model [27].

the heat distribution for the front and rear ellipsoids (Fig. 5) were calculated separately as follows [27]:

$$q_f(x,y,z) = \frac{6\sqrt{3}\eta Q f_f}{\pi\sqrt{\pi}a_f bc}\exp\left(-\frac{3x^2}{b^2}-\frac{3y^2}{c^2}-\frac{3z^2}{a_f{}^2}\right) \quad (1)$$

$$q_r(x,y,z) = \frac{6\sqrt{3}\eta Q f_r}{\pi\sqrt{\pi}a_r bc}\exp\left(-\frac{3x^2}{b^2}-\frac{3y^2}{c^2}-\frac{3z^2}{a_r{}^2}\right) \quad (2)$$

where, a_f, a_r, b, and c are the dimensional constants of the Goldak's model, $Q = VI$ is the total heat input, η is the thermal efficiency which is assumed to be 60% for the GTAW process [28], and f_f and f_r are the heat fraction coefficients in the front and rear ellipsoids, respectively, $f_f + f_r = 2$ [27]. In this study, a_f, a_r, b, and c are considered 4, 12, 4, and 2 mm, respectively and f_f and f_r are 1.5 and 0.5.

3.3 Mechanical analysis

Total strain rate during welding is decomposed into the four components [29]:

$$\dot{\varepsilon}_t = \dot{\varepsilon}_e + \dot{\varepsilon}_p + \dot{\varepsilon}_{th} + \dot{\varepsilon}_{pt} \quad (3)$$

where $\dot{\varepsilon}_e$, $\dot{\varepsilon}_p$, $\dot{\varepsilon}_{th}$, and $\dot{\varepsilon}_{pt}$ are the elastic, plastic, thermal, and solid-state phase transformation strain rates, respectively.

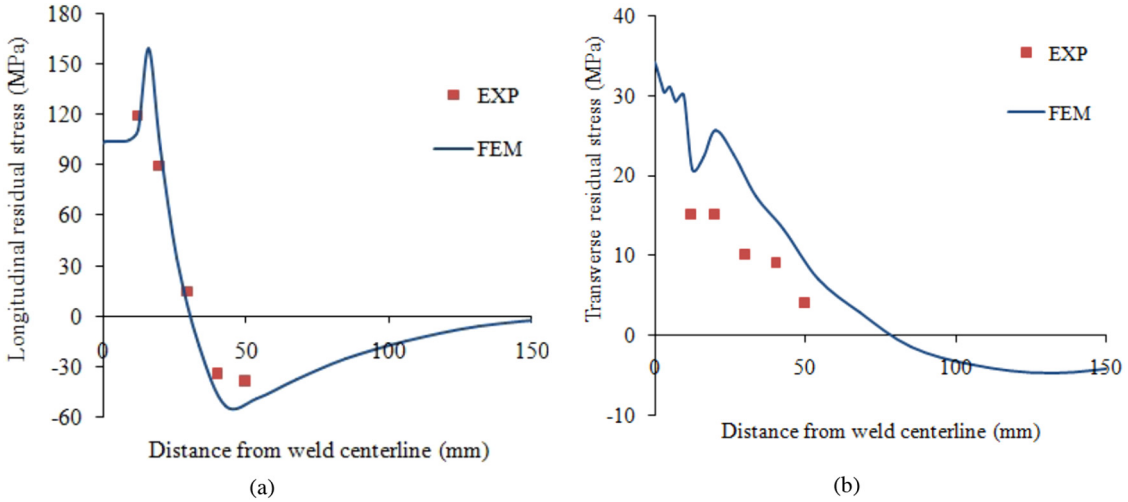

Fig. 6. (a) Longitudinal and (b) transverse residual stress distributions.

During welding of the 5000 series-aluminum, solid-state phase transformation does not occur, so $\dot{\varepsilon}_{pt}$ is ignored.

3.4 Result of welding simulation

Figure 6 shows the predicted and the measured residual stresses. The stresses were extracted from the midsection perpendicular to the weld line. As seen, the maximum longitudinal residual stress (160 MPa) equals to the yield strength, approximately. Whereas, the maximum transverse residual stress (34 MPa) is much lower than the yield strength. Hence, a good agreement was found between the test and the FE analysis.

4 Simulation of the welding residual stress relaxation under cyclic loading

4.1 Plastic constitutive model

By using the von Mises criterion, the yield function can be expressed as [30]:

$$f = \sqrt{3/2(\sigma_D - X_D)\colon(\sigma_D - X_D)} - \sigma_0 - R \qquad (4)$$

where, σ_D is the deviatoric part of the stress tensor, X_D is the deviatoric part of the back stress, σ_0 is the initial yield stress, and R is the isotropic hardening variable.

4.1.1 Isotropic hardening

The isotropic hardening (IH) assumes the uniform expansion without translation of the yield surface within the stress space, which can be explained by the following equation [30]:

$$R = q\left(1 - e^{-bp}\right) \qquad (5)$$

where, p is the equivalent plastic strain, b determines the rate of isotropic hardening change, and q is the maximum change in the size of the yield surface.

4.1.2 Nonlinear kinematic hardening

The kinematic hardening assumes that the yield surface translates in the stress space without any expansion. The nonlinear kinematic hardening model (NLKH) can be expressed as [31]:

$$dX = C(\sigma_D - X)dp - \gamma X dp \qquad (6)$$

where, C and γ are the material parameters describing the nonlinear kinematic hardening. ABAQUS software provides a method to directly implement the combined isotropic and kinematic hardening model using empirical data of cyclic strain-controlled test and static tensile test [32].

4.2 Cyclic plasticity response

The low cycle fatigue (LCF) tests were performed based on the ASTM E606 standard [33] to characterize the cyclic hardening properties. The strain-controlled tests were carried out on flat specimens by a servo-hydraulic testing machine with 100 KN capacity (Fig. 7), sinusoidal wave shape, and frequency of 1 Hz. The cyclic stress–strain curves were determined using the companion test method. This method requires a series of test specimens, which each specimen is subjected to a constant strain amplitude [34]. The tests were carried out on each specimen until it fractured in two parts. Figure 8 shows the variation of stress amplitude with the number of cycles for strain ranges of 1.1%, 1.2%, and 1.9%. As seen, the material presents significant hardening due to cyclic loading.

4.3 FE analysis with cyclic loading

To study the plasticity behavior on the residual stress relaxation, two different plasticity constitutive models were implemented into the FE analysis: (1) perfect plasticity without hardening (NH), and (2) combined isotropic hardening with nonlinear kinematic hardening

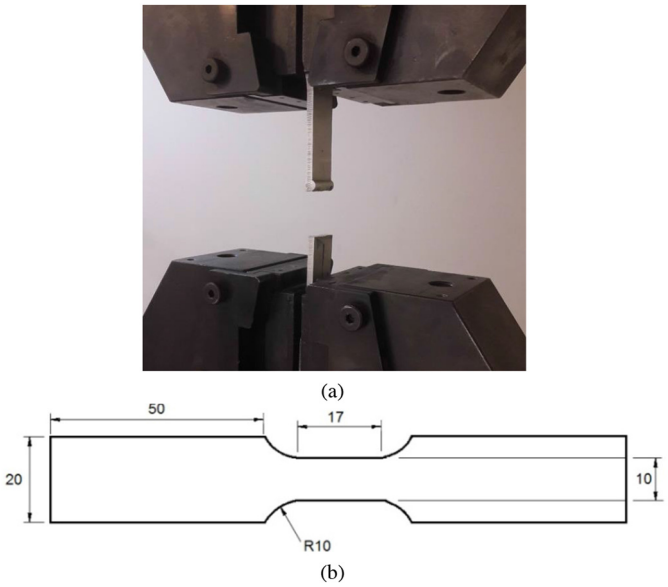

Fig. 7. LCF tests (a) experimental setup (b) specimen geometry [33].

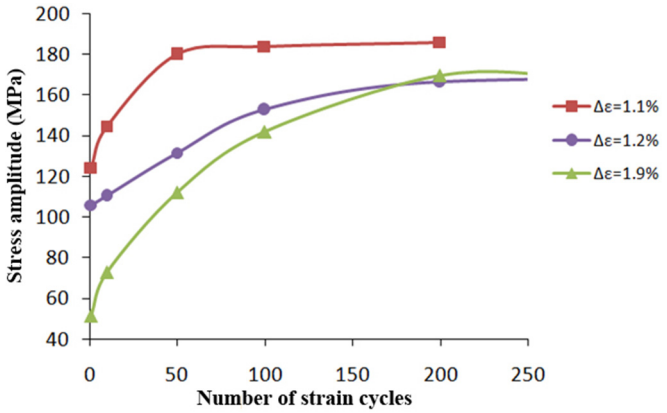

Fig. 8. Variation of stress amplitude with number of cycles.

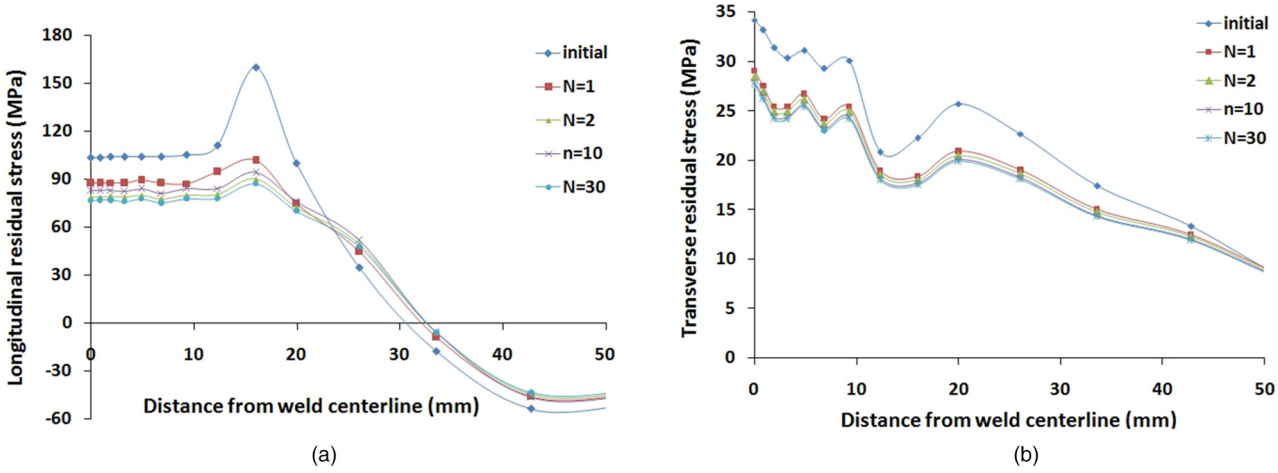

Fig. 9. (a) Longitudinal, (b) transverse residual stress distributions after cyclic loading with $Sa = 100$ MPa for NH model.

(IH&NLKH). In this analysis, the same FE model of the welding simulation was used, except that the boundary condition and the loading were modified. The residual stress field determined in previous section was used as the initial load. The fully reversed cyclic loading, parallel to the weld line, was applied to the one end of the plate and the other end was fixed.

Figures 9 and 10 show the longitudinal and transverse residual stress distributions after different number of cycles with the load amplitude $Sa = 100$ MPa for NH and IH&NLKH models, respectively. As can be seen, for both plasticity models the tensile residual stress in the longitudinal and the transverse directions will be decreased by the cyclic loading. However, the relaxation is limited to the initial cycle, which the residual stress stabilized after that, i.e. the subsequent cycles do not contribute to the relaxation significantly. In addition, the stress relaxation along the longitudinal direction is greater than that along the transverse direction.

Figures 11 and 12 show the stabilized longitudinal residual stresses at different load amplitudes for NH and IH&NLKH models, respectively. As seen, the external cyclic load causes redistribution in the welding residual stress. It can be concluded that the amount of relaxation depends on the level of applied cyclic load, i.e. a higher load amplitude results in a greater residual stress change.

Figure 13 shows the percentage reduction of the longitudinal residual stress due to relaxation versus to the load amplitude (data is extracted at a distance of 16 mm from weld centerline). This figure indicates that the NH model causes a greater stress relaxation than the IH&NLKH model. The reason is that the magnitude of the stress relaxation depends on the accumulated plastic strain, which is stronger in the perfectly plastic model. Experiments have shown that the 5000-series aluminums exhibit cyclic strain hardening with the Bauschinger effect [35]. However, the perfectly plastic model assumes no strain hardening in tension and compression; the initial yield

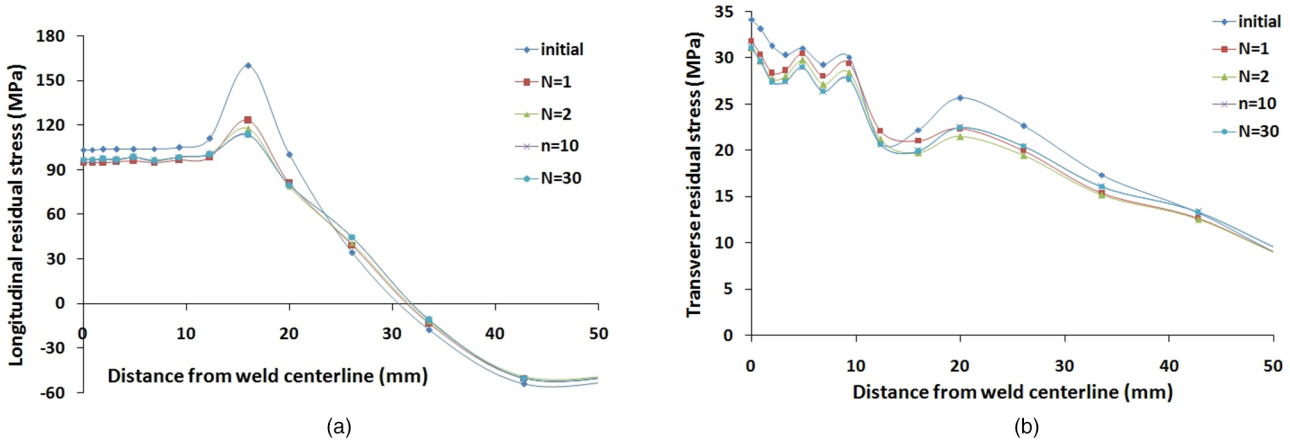

Fig. 10. (a) Longitudinal, (b) transverse residual stress distributions after cyclic loading with $Sa = 100$ MPa for IH&NLKH model.

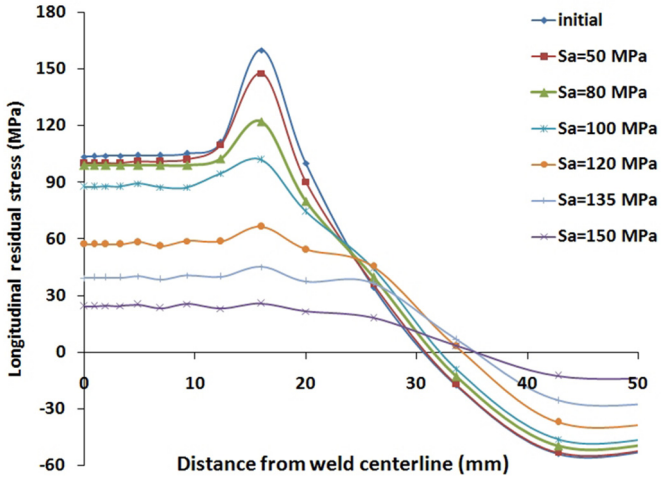

Fig. 11. Stabilized longitudinal residual stress at different load amplitude for NH model.

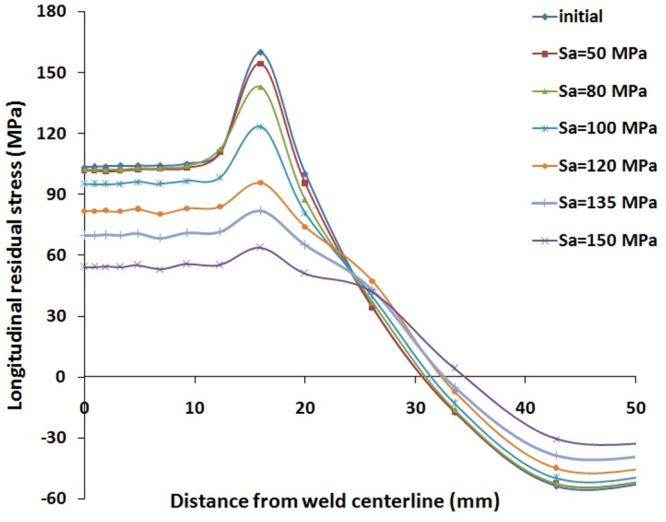

Fig. 12. Stabilized longitudinal residual stress at different load amplitude for IH&NLKH model.

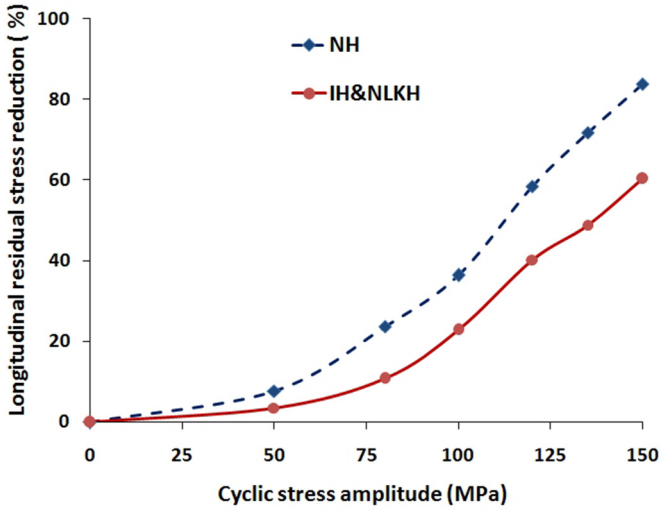

Fig. 13. Percentage reduction of longitudinal residual stress versus to load amplitude.

function is unchanged in the stress space during plastic deformation. Therefore, to more accurate assessment of the welding residual stress relaxation in aluminum-welded plates, the IH&NLKH model should be used, which will be utilized in the subsequent section.

5 Design of experiments

Since there are many effective parameters on the welding residual stress relaxation, design of experiments based on the Taguchi method [36] was done to study the impact of main parameters. The characteristics of the cyclic load consist of stress amplitude (S_a), mean stress (S_m), and number of cycles (N) were selected as the loading parameters, and the maximum von Mises of the initial welding residual stress (σ_{Irs}) was selected as the technological parameter. Based on the number of design factors and their levels, the Taguchi L18 array was used in the experimental design, as shown in Table 3. The maximum von Mises of the residual stresses after applying the cyclic

Table 3. Design factors and their levels.

Experiment no.	N	S_m (MPa)	S_a (MPa)	σ_{Irs} (MPa)
1	1	30	20	110
2	1	60	40	135
3	1	90	60	150
4	2	30	20	135
5	2	60	40	150
6	2	90	60	110
7	4	30	40	110
8	4	60	60	135
9	4	90	20	150
10	8	30	60	150
11	8	60	20	110
12	8	90	40	135
13	16	30	40	150
14	16	60	60	110
15	16	90	20	135
16	32	30	60	135
17	32	60	20	150
18	32	90	40	110

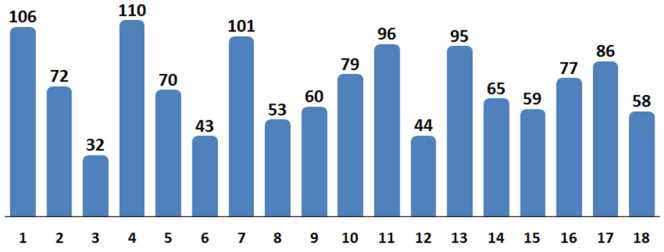

Fig. 14. Relaxed residual stresses for all experiments (MPa).

loading, namely relaxed residual stress, (σ_{Rrs}) was selected as the response variable. Using the FE analysis, the response variable values were determined for all experiments, as plotted in Figure 14.

5.1 Taguchi analysis

The results of the Taguchi analysis are given in Table 4. This table presents the averages of the relaxed residual stresses for every level of design factors. Delta is the maximum difference of response variable between the levels of each factor, and Rank specifies the rank of each factor based on the Delta values. As seen, the order of factors based on their effects on the relaxed residual stress is determined as follows: mean stress, stress amplitude, initial residual stress, and finally number of cycle. This can be also observed in the plot of design factor impacts shown in Figure 15. As seen, the mean stress and the stress amplitude causes the relaxed residual stress to reduce, while the effect of the number of cycles is rather insignificant.

Table 4. Average values of relaxed residual stresses in every level of each factor (MPa).

Level	N	S_m	S_a	σ_{Irs}
1	74.1	94.6	86.4	78.8
2	73.5	73.8	73.2	69.1
3	73.3	49.4	58.2	70.5
4	73.1	–	–	–
5	73.3	–	–	–
6	73.2	–	–	–
Delta	1.1	45.1	28.1	9.1
Rank	4	1	2	3

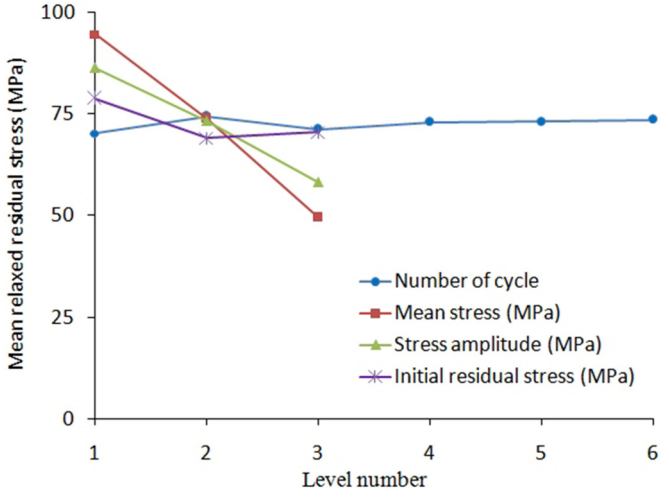

Fig. 15. Design factor effects on the relaxed residual stress.

5.2 Regression analysis

The regression analysis was performed to derive the relationship between the design factors and the response variable. By this analysis, the relaxed residual stress was estimated through the following first order equation,

$$\sigma_{Rrs} = 172.7 - 0.0153N - 0.7522S_m - 0.7031S_a - 0.2083\sigma_{Irs}, \quad R^2 = 97.5\%. \tag{7}$$

In equation (7), each numerical coefficient reveals the importance of the corresponding parameter. In addition, the negative sign of coefficients declares reduction of the relaxed residual stress. In this study, the high value of R^2 (variation percentage of the response) indicates that the fit of the experimental data to the model is satisfactory.

5.3 Analysis of variance

Analysis of variance (ANOVA) was then carried out to interpret the results of the experiments and detect

the amount of contribution of each variable. The ANOVA result for the first order regression is shown in Table 5. The sum of squares indicates the relative importance of each factor; the factor with the biggest sum of squares has the greatest impact. The p-value also shows the significance level of each factor; a smaller p-value corresponds to a greater significance. Table 5 indicates that mean stress ($p = 0$), stress amplitude ($p = 0$), initial residual stress ($p = 0.004$), and number of cycles ($p = 0.56$) in this order are the most significant factors affecting the relaxed residual stress. Moreover, mean stress with 68.5% contribution has the most impact on the relaxed residual stress. Notice that these conclusions are consistent with the Taguchi analysis results.

Figure 16 shows the residual plots for the proposed first order equation. This figure can be used to asses if the model satisfies the assumptions of the analysis. A residual is the difference between an observed value and its corresponding fitted value. The normal probability plot approximately follows a straight line. This means that the data are normally distributed. Histogram of the residuals also indicates that the data is not skewed and normally disturbed. In addition, the residual versus order plot displays no pattern in distribution of data, which indicates that the residual values are independent of each other.

In order to verify the regression analysis, the results of the FE method were compared with the values derived from equation (7) as shown in Table 6. As seen, the maximum relative difference is 12%. This is compatible with the residual plots.

Table 5. ANOVA results for the first order regression.

Source	Sum of squares	p-value	Contribution
N	6	0.56	0.07%
S_m	6110	0	68.5%
S_a	2373	0	26.6%
σ_{Irs}	213	0.004	2.4%
Error	–	–	2.4%

6 Conclusions

This paper studied the influence of the main parameters on the residual stress relaxation of aluminum welded-plates under cyclic loading. The induced residual stress for the welded plates was predicted using FE analysis. The experimental residual stress measurements are in good agreement with the predicted stresses. To study the plasticity effect on the stress relaxation, two different models were considered: perfect plasticity, and combined nonlinear isotropic-kinematic hardening. In addition, the effect of various loading and technological parameters on the stress relaxation was studied through the Taguchi method. In summary, the following conclusions can be drawn from this research:

– The residual stress relaxation is highly dependent on the plasticity behavior. The NH causes to a greater relaxation compared to IH&NLKH.
– The IH&NLKH model successfully predicts the redistribution of welding residual stress in a strain hardening aluminum due to its ability to precisely determine the accumulated plastic strain.

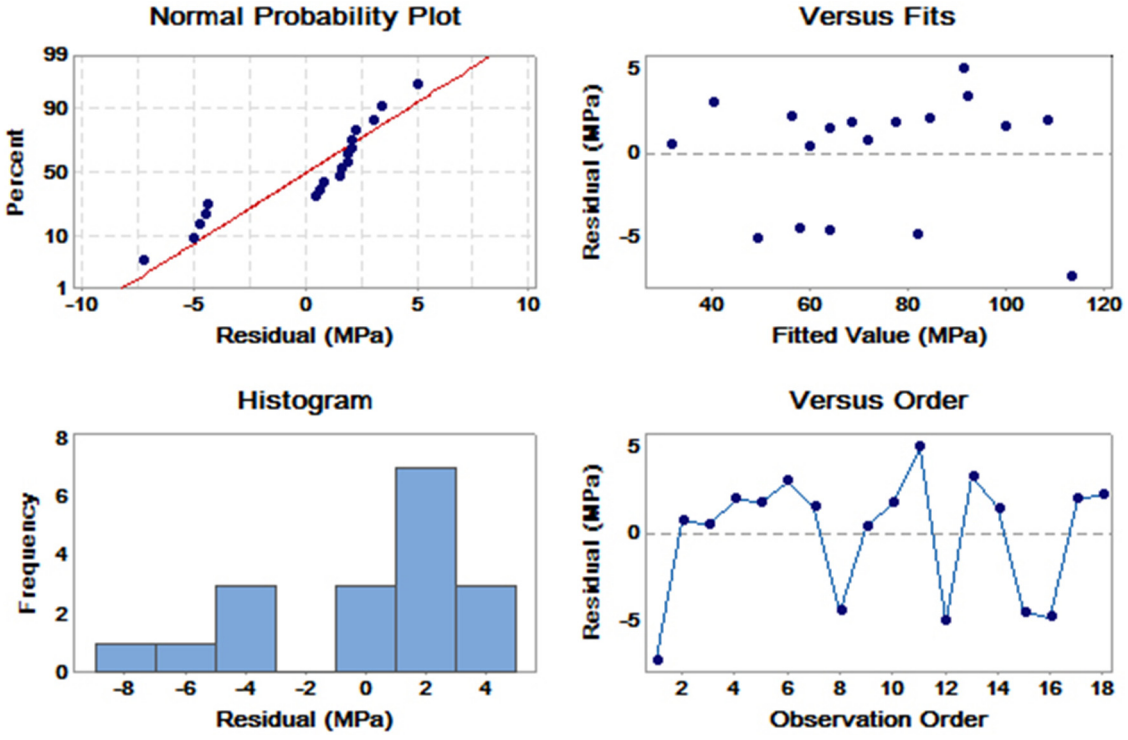

Fig. 16. Residual plots for the first order regression.

Table 6. Comparison between the results of the FEM and the model (MPa).

Experiment no.	FEM	Equation (7)	Difference (%)
1	106	113	6
2	72	71	−1
3	32	32	−1
4	110	108	−2
5	70	68	−3
6	43	40	−8
7	101	99	−2
8	53	57	8
9	60	60	−1
10	79	77	−2
11	96	90	−6
12	44	49	12
13	95	91	−4
14	65	62	−5
15	59	63	7
16	77	79	3
17	86	82	−5
18	58	53	−8

– The residual stress is stabilized after the first cycle and the amount of stress relaxation occurred in subsequent cycles is insignificant.
– Increase in the mean stress and the stress amplitude cause the stress relaxation to increase, while the effect of number of cycles is rather insignificant
– The most significant factors on welding residual stress relaxation in the order of significance are the following: the mean stress, the stress amplitude, the initial residual stress, and the number of cycles.

Nomenclature

a_f, a_r, b, c	Dimensional constants of the Goldak's model (mm)
b	Rapidity of isotropic hardening change
C	Nonlinear kinematic hardening parameter (MPa)
f	Von Mises yield function (MPa)
f_f, f_r	Heat fraction in front and rear ellipsoids of the Goldak's model
N	Number of cycles
p	Equivalent plastic strain
p-value	Probability value
q	Saturated value of isotropic hardening (MPa)
Q	Total heat power of welding source (W)
R	Isotropic hardening value (MPa)
S_a,S_m	Stress amplitude and mean stress (MPa)
X_D	Deviatoric part of back stress tensor (MPa)
γ	Nonlinear kinematic hardening parameter
$\dot{\varepsilon}_e$, $\dot{\varepsilon}_p$, $\dot{\varepsilon}_{th}$, $\dot{\varepsilon}_{pt}$	Elastic, plastic, thermal, and phase transformation strain rates
η	Thermal efficiency of welding heat source
σ_0	Initial yield stress (MPa)
σ_D	Deviatoric part of the stress tensor (MPa)
σ_{Irs}, σ_{Rrs}	Von Mises values of initial and relaxed welding residual stresses (MPa)

Conflict of interest

The authors declare that they have no conflict of interest.

Funding

This research did not receive any specific grant.

References

[1] J. Klassen, N. Friedrich, W. Fricke, T. Nitschke-Pagel, K. Dilger, Influence of residual stresses on fatigue strength of large-scale welded assembly joints, Weld. World **61**, 361–374 (2017)
[2] I. Vysotskiy, S. Malopheyev, S. Rahimi, S. Mironov, R. Kaibyshev, Unusual fatigue behavior of friction-stir welded Al–Mg–Si alloy, Mater. Sci. Eng. A **760**, 277–276 (2019)
[3] D. Wang, H. Zhang, B. Gong, C. Deng, Residual stress effects on fatigue behavior of welded T-joint: a finite fracture mechanics approach, Mater. Des. **91**, 211–217 (2016)
[4] Y. Javadi, K. Azari, S.M. Ghalehbandi, M.J. Roy, Comparison between using longitudinal and shear waves in ultrasonic stress measurement to investigate the effect of post-weld heat-treatment on welding residual stresses, Res. Nondestruct. Eval. **28**, 101–122 (2015)
[5] Z. Zhang, P. Ge, G.Z. Zhao, Numerical studies of post weld heat treatment on residual stresses in welded impeller, Int. J. Pres. Ves. Pip. **153**, 1–14 (2017)
[6] C. Bianchetti, D. Delbergue, P. Bocher, M. Lévesque, M. Brochu, Analytical fatigue life prediction of shot peened AA 7050-T7451, Int. J. Fatigue **118**, 271–281 (2019)
[7] Y. Gao, Improvement of fatigue property in 7050-T7451 aluminum alloy by laser peening and shot peening, Mater. Sci. Eng. A **528**, 3823–3828 (2011)
[8] J. Liu, H. Yuanb, Prediction of residual stress relaxations in shot-peened specimen sand its application for the rotor disc assessment, Mater. Sci. Eng. A **527**, 6690–6698 (2010)
[9] V.I. Trufyakov, Y.F. Kudyavtsev, Calculation of the effect of external loading on the relaxation of residual welding stresses, Weld. Int. **3**, 22–24 (2010)
[10] O.S. Zaroog, A. Ali, B.B. Sahari, R. Zahari, Modeling of residual stress relaxation of fatigue in 2024-T351 aluminum alloy, Int. J. Fatigue **33**, 279–285 (2011)
[11] J. Katsuyama, K. Onizawa, Analytical study of the relaxation of welding residual stress by excessive loading for austenitic stainless steel piping welds, J. Pressure Vessel Technol. **133**, 417–424 (2011)
[12] H. Yi, Y. Lee, Numerical analysis of welding residual stress relaxation in high-strength multilayer weldment under fatigue loads, Metall. Mater. Trans. B **48**, 2167–2175 (2017)

[13] Z. Barsoum, I. Barsoum, Residual stress effects on fatigue life of welded structures using LEFM, Eng. Fail. Anal. **16**, 449–467 (2009)
[14] J. Katsuyama, K. Onizawa, Analytical study of the relaxation of welding residual stress by excessive loading for austenitic stainless steel piping welds, J. Pressure Vessel Technol. **133**, 031402 (2011)
[15] J. Katsuyama, Y. Yamaguchi, Y. Li, K. Onizawa, Effect of cyclic loading on the relaxation of residual stress in the butt-weld joints of nuclear reactor piping, Nucle. Eng. Des. **278**, 222–228 (2014)
[16] V. Dattoma, M. De Giorgi, R. Nobile, Numerical evaluation of residual stress relaxation by cyclic load, J. Strain Anal. Eng. **39**, 663–672 (2004)
[17] Z. Qian, S. Chumbley, T. Karakulak, E. Johnson, The residual stress relaxation behavior of weldments during cyclic loading, Metall. Mater. Trans. A **44A**, 3147–3156 (2013)
[18] L.G. Gannon, N.G. Pegg, M.J. Smith, Y. Liu, Effect of residual stress shakedown on stiffened plate strength and behaviour, Ships Offshore Struct. **8**, 638–652 (2013)
[19] J. Cho, C.H. Lee, FE analysis of residual stress relaxation in a girth-welded duplex stainless steel pipe under cyclic loading, Int. J. Fatigue **82**, 462–473 (2016)
[20] C.H. Lee, N.V. Van Do, K.H. Chang, Analysis of uniaxial ratcheting behavior and cyclic mean stress relaxation of a duplex stainless steel, Int. J. Plast. **62**, 17–33 (2014)
[21] X.F. Xie, W. Jiang, Y. Luo, S. Xu, J.M. Gong, S.T. Tu, A model to predict the relaxation of weld residual stress by cyclic load: Experimental and finite element modeling, Int. J. Fatigue **95**, 293–301 (2017)
[22] M. Farajian-Sohi, T. Nitsckhe-Pagel, K. Dilger, Mechanisms of residual rtress relaxation and redistribution in welded high-strength steel specimens under mechanical loading, Weld. Word **54**, R366–R374 (2010)
[23] M. Farajian-Sohi, T. Nitsckhe-Pagel, K. Dilger, Residual stress relaxation of quasi-statically and cyclically loaded steel welds Doc. IIW-1980-08 (ex-doc. XIII-2219-08), Weld. World **54**, R49–R60 (2010)
[24] ASME Boiler and pressure vessel code: section II- part D properties (ASME, New York, 2015)
[25] ASTM E 21–09: Standard test methods for elevated temperature tension tests of metallic materials (ASTM International, New York, 2009)
[26] Y. Javadi, M.C. Smith, K. Abburi Venkata et al., Residual stress measurement round robin on an electron beam welded joint between austenitic stainless steel 316L(N) and ferritic steel P91, Int. J. Pres. Ves. Pip. **154**, 41–57 (2017)
[27] Y. Javadi, J.A. GoldakA, K. Imani Fooladi, M. Nimrouzi, Using ultrasonic and finite element for residual stress evaluation of a gas transmission pipeline, Mater. Eval. **76**, 192–202 (2018)
[28] N. Stenbacka, I. Choquet, K. Hurtig, Review of arc efficiency values for gas tungsten arc welding, IIW Commission IV-XII-SG212, Berlin, Germany, 2012, pp. 1–21
[29] G. Fu, M.I. Lourenço, M. Duan, S.F. Estefen, Influence of the welding sequence on residual stress and distortion of fillet welded structures, Mar. Struct. **46**, 30–55 (2016)
[30] A. Nath, K.K. Ray, S. Barai, Evaluation of ratcheting behaviour in cyclically stable steels through use of a combined kinematic-isotropic hardening rule and a genetic algorithm optimization technique, Int. J. Mech. Sci. **152**, 138–150 (2019)
[31] S. Yun, A. Palazotto, Damage mechanics incorporating two back stress kinematic hardening constitutive models, Eng. Fract. Mech. **74**, 2844–2863 (2007)
[32] ABAQUS analysis user's manual, version 6.12
[33] ASTM E606/E606M: Standard test method for strain-controlled fatigue testing (ASTM, New York, 2012)
[34] R.I. Stephens, A. Fatemi, R.R. Stephens, H.O. Fuchs, Metal Fatigue in Engineering, 2nd edn. (John Wiley & Sons, New York, 2000)
[35] F. Lu, G. Kang, Y. Liu, K. Shi, Experimental study on uniaxial cycle deformation of rolled 5083AL alloy plate. 7th ICLCF 87–93, Aachen, Germany, 2013
[36] R.K. Roy, Design of Experiments Using the Taguchi Approach: 16 Steps to Product and Process IMPROVEMENT (John Wiley & Sons, New York, 2001)

Cite this article as: Y. Ghaderi Dehkordi, A. Pourkamali Anaraki, A.R. Shahani, Comparative study of the effective parameters on residual stress relaxation in welded aluminum plates under cyclic loading, Mechanics & Industry **21**, 505 (2020)